

Placing limits on the transit timing variations of circumbinary exoplanets

D. Armstrong,¹* D. V. Martin,² G. Brown,¹ F. Faedi,¹ Y. Gómez Maqueo Chew,^{1,3}
R. Mardling,^{2,4} D. Pollacco,¹ A. H. M. J. Triaud^{2,5}† and S. Udry²

¹Department of Physics, University of Warwick, Gibbet Hill Road, Coventry CV4 7AL, UK

²Observatoire de Genève, Université de Genève, 51 chemin des Maillettes, CH-1290 Sauverny, Switzerland

³Department of Physics and Astronomy, Vanderbilt University, Nashville, TN 37235, USA

⁴School of Mathematical Sciences, Monash University, Vic 3800, Australia

⁵Department of Physics, and Kavli Institute for Astrophysics and Space Research, Massachusetts Institute of Technology, Cambridge, MA 02139, USA

Accepted 2013 July 1. Received 2013 June 28; in original form 2013 May 15

ABSTRACT

We present an efficient analytical method to predict the maximum transit timing variations of a circumbinary exoplanet, given some basic parameters of the host binary. We derive an analytical model giving limits on the potential location of transits for coplanar planets orbiting eclipsing binaries, then test it against numerical N -body simulations of a distribution of binaries and planets. We also show the application of the analytic model to Kepler-16b, -34b and -35b. The resulting method is fast, efficient and is accurate to approximately 1 per cent in predicting limits on possible times of transits over a 3-yr observing campaign. The model can easily be used to, for example, place constraints on transit timing while performing circumbinary planet searches on large data sets. It is adaptable to use in situations where some or many of the planet and binary parameters are unknown.

Key words: binaries: eclipsing – planetary systems.

1 INTRODUCTION

To date seven transiting circumbinary exoplanets have been discovered, all from the NASA *Kepler* mission data (Doyle et al. 2011; Orosz et al. 2012a,b; Schwamb et al. 2012; Welsh et al. 2012). Such circumbinary planets provide interesting tests of planet formation theories, having formed in a complex environment. Recently several studies have been performed on their formation (e.g. Gong, Zhou & Xie 2012; Meschiari 2012a,b; Pelupessy & Zwart 2012), orbital stability (e.g. Pichardo, Sparke & Aguilar 2005, 2008; Doolin & Blundell 2011; Jaime, Pichardo & Aguilar 2012) and variations in insolation from a habitability perspective (e.g. Kane & Hinkel 2012; O'Malley-James et al. 2012). They are beginning to be subjected to analytical models, such as that provided by Leung & Lee (2013, hereafter LL). Such planets are valuable objects for our understanding of planetary formation and evolution, with further discoveries needed to provide observational constraints on these interesting and complex systems. Their signal may be present in data sets from other transit surveys such as Wide Angle Search for Planets (WASP; Pollacco et al. 2006) or Next Generation Transit Survey (NGTS; Wheatley et al. 2013). Detecting these planets via the transit method presents observational challenges, as they exhibit

transit timing variations (TTVs) on the order of days in magnitude, in addition to changes in the shape and duration of transits.

The purpose of this paper is to present constraints on the observational characteristics of a transiting circumbinary exoplanet through our knowledge of the host binary system, using a fast method which requires no complex modelling. In this way we aim to aid detection through reducing the problems generated by the large-scale TTVs mentioned above. Specifically we address TTVs in coplanar circumbinary systems, placing general limits on the magnitude of such variations, through constraining the location of possible transits. A similar analysis was carried out for the system KIC 002856960 (Armstrong et al. 2012; Lee et al. 2013), which shows similar large-scale TTVs, and multiple transits per orbit, albeit in a triple star scenario. These constraints are of use to surveys for such planets, where we can place limits on and aid the design of new automated searches, such as the Quasiperiodic Automated Transit Search (QATS) algorithm (Carter & Agol 2013). While it is possible with numerical simulations to predict exact times of transit for circumbinary systems, our analytical model allows (under some approximations) constraints to be placed on systems where some or many orbital parameters are not yet known, including the majority of eclipsing binaries in the Kepler Eclipsing Binary Catalogue (Prsa et al. 2011; Slawson et al. 2011).

TTVs on the transits of circumbinary planets have two main sources. The first is a geometrical timing variation (we refer to this as Effect I) resulting from the changing positions of the host binary stars. This leads to a range in time in which transits can occur,

*E-mail: d.j.armstrong@warwick.ac.uk

†Fellow of the Swiss National Science Foundation.

similar to more ‘usual’ TTVs, and is derived in Section 2.1.1. The second is a precessional variation (referred to as Effect II), a long-term oscillation in time around a constant periodicity of the potential location of transits, caused by precession of the planet’s orbit (which is itself caused by torques arising from the non-point mass nature of the binary). It is treated in Section 2.1.2. There are other possible sources of TTVs, such as another planet in the system. The effect of such a planet, or any other known source of TTVs, is negligible compared to the above in circumbinary systems (cf. Kepler-47b,c where planet–planet interactions are negligible; Orosz et al. 2012b).

We make use of several unusual terms in this paper, and define them here for clarity. First, a ‘crossing’, or ‘crossing region’. This is the region of a circumbinary exoplanet’s orbit where the planet crosses the binary star orbit, from the observer’s perspective. It may only transit the stars within this crossing region, but will generally spend most of its time in the region out of transit. Second, we use extensively the ‘azimuthal’ period of a circumbinary planet, mentioned in LL. There are several periods which may be relevant to a circumbinary planet, and we make use of two here – the azimuthal period and the Keplerian period. The azimuthal period is the period which on average the planet takes between successive alignments with the observer, i.e. to traverse 2π rad relative to a fixed reference vector and plane. The Keplerian period is an osculating period taken at a particular epoch, derivable from Kepler’s third law via the binary mass and planet semimajor axis. These two periods are not equivalent, and are discussed further in Section 4.

The structure of the paper is as follows. Section 2.1 describes a Keplerian approximation which can be used to estimate the possible location of transits for a general planet and binary. Section 2.2 describes the implementation of a numerical model used to test this approximation, with application to a demonstration simulated system. Section 3 shows the results of testing the analytical model against a distribution of binaries and planets modelled numerically, and applies the models to Kepler-16b, -34b and -35b. Section 4 discusses the accuracy and usefulness of these results, as well as discussing observational issues in the search for circumbinary transiting exoplanets.

2 MODELS

2.1 Analytic approximation

We present here a derivation which allows the potential location of transits of a circumbinary planet to be estimated without the need for detailed modelling or any free parameters. It proceeds using Keplerian orbital equations for both the stars and planets of a circumbinary system, and hence is an approximation only, as it does not consider three-body effects that perturb the orbits of the binary and planet (although precession of the planet’s argument of periapse is included). We consider the TTVs of transits of only one star at a time, through this paper star 1. To consider transits of star 2, swap the indices 1 and 2 in equation (3).

2.1.1 Geometrical timing variations – Effect I

These variations arise from the movement of the binary stars within their orbit. As such we use the limits of this orbit, coupled with the time the planet takes to cross said orbit. We make use of an equation for the duration of a transit in a single star/planet system (equation 1, from Winn 2010, their equation 14). A crossing (defined in Section 1) of a circumbinary planet is analogous to the transit

of a single star by a planet passing in front of it; conceptually, we just replace the single star with a ‘metastar’ of diameter equal to the maximum extent of the binary’s orbit, giving

$$T_{\text{GTV}} = \frac{P_p}{\pi} \arcsin \left(\frac{R_{\text{metastar}}}{a_p} \right) \frac{\sqrt{1 - e_p^2}}{1 + e_p \sin(\omega_p)}, \quad (1)$$

where T_{GTV} represents the duration of the crossing, subscript ‘p’ represents the planet, P the azimuthal period, a the semimajor axis, e the eccentricity and ω the argument of periapse. We have made the approximation that the impact parameter $b_p \ll R_{\text{metastar}}$, the inclination of the planet $i_p = \pi/2$ and $R_p \ll R_{\text{metastar}}$. To find R_{metastar} we must derive the extent of the binary’s orbit, projected on to the sky.

Consider the eclipsing binary orbit to be in the x - z plane, with the z -axis being along the line of site of the observer. By doing this we take the binary orbit to have inclination $\pi/2$, a reasonable approximation for detached eclipsing binaries and for this purpose. Take the motion of star 1 in the x plane, projected on to the sky. From Murray & Correia (2010b, their equation 53, with $\Omega = 0$), this is given by

$$X = \beta(f) a_b, \quad (2)$$

where

$$\beta(f_b) = \frac{M_2}{M_1 + M_2} \frac{(1 - e_b^2)}{1 + e_b \cos(f_b)} \cos(\omega_b + f_b), \quad (3)$$

and subscript ‘b’ represents the binary, f the true anomaly and $M_{1,2}$ the mass of stars 1 and 2, respectively. Taking the zero-points of the differential with respect to f_b of equation (2) gives us the minimum and maximum values of X – the extent of the star’s motion projected on to the sky. The values of the true anomaly of the binary at these points are given by

$$f_0, f_1 = \arcsin[-e_b \sin(\omega_b)] - \omega_b. \quad (4)$$

Equation (4) has two solutions within the range $0, 2\pi$. Inserting both into equation (2) gives the maximum and minimum values for X . We term these X_1 and X_0 . Which of X_0 and X_1 is the minimum and which the maximum depends on ω_b , but is unimportant here.

The radius of the ‘metastar’ is given by

$$R_{\text{metastar}} = \frac{|X_1| + |X_0|}{2}, \quad (5)$$

and a scaled radius by

$$R_{\text{m,scaled}} = \frac{R_{\text{metastar}}}{a_b} = \frac{|\beta(f_1)| + |\beta(f_0)|}{2}. \quad (6)$$

Substituting equation (5) into equation (1) leads to

$$T_{\text{GTV}} = \frac{P_p}{\pi} \arcsin \left[R_{\text{m,scaled}} \left(\frac{P_b}{P_p} \right)^{\frac{2}{3}} \right] \frac{\sqrt{1 - e_p^2}}{1 + e_p \sin(\omega_p)}, \quad (7)$$

where the ratio of semimajor axes has been substituted to the equivalent ratio of periods using Kepler’s third law, allowing the use of the azimuthal period outlined in Section 1. In the presented form T_{GTV} represents the duration of a crossing, and as such a range of time within which transits can occur. The argument of periapse, ω_p , is a function of time due to precession of the planetary orbit; assuming a constant precession rate it can be estimated analytically using equation (5) of Doolin & Blundell (2011, hereafter DB), which is derived from that of Farago & Laskar (2010).

Lacking knowledge of the present system alignment, it is possible to take a ‘safe’ approximation by using the value of ω_p which gives

the maximum T_{GTV} , i.e. $\omega_p = 3\pi/2$. This corresponds to when the planet transits near its apoapse, and hence is travelling relatively slowly so that the range of transit times is extended. Using this constant value of T_{GTV} is often more practical. For systems with low planetary eccentricity the variation caused by varying ω_p is small (on the order of a few per cent in T_{GTV}).

2.1.2 Precessional timing variation – Effect II

This variation is caused by the precession of the planet’s orbit. For an eccentric planetary orbit, this precession will result in shifts in the time of potential transits away from the ‘expected’ time for a constant periodic signal. The magnitude of these shifts at a given time depends on the instantaneous value of ω_p .

We assume a constant precession rate for the planetary orbit, such that

$$\frac{d\omega_p}{dt} = \frac{2\pi}{P_\omega}, \quad (8)$$

where P_ω represents the period of precession of the planet’s periapse, and can be estimated analytically through the equation of DB.

For a planet precessing in the prograde direction, this change in ω_p represents time ‘gained’, a portion of its orbit which it does not have to cover before aligning with the observer once more. The differential amount of time saved (i.e. period shifted) in this way is given by

$$\frac{dP_p}{d\omega_p} = \frac{dt}{df_p}, \quad (9)$$

where dP represents an apparent change in the period of the planet, and f_p is the true anomaly of the planet, with dt/df_p evaluated at $f_p = \pi/2 - \omega_p$, the value of f_p at transit conjunction.

There are two contributions here, a constant term from the precession and a varying oscillation induced by the effect of the eccentricity of the planet’s orbit. The constant term can be found simply, by realizing that the planet ‘loses’ one full orbit of time in one precessional period. For a constant precession rate, this gives a constant rate of time loss of P_p/P_ω , which must be subtracted from equation (9) to find the oscillation term. When using the azimuthal period of the planet (as defined in Section 1), or searching observationally for transits this constant term is automatically accounted for, which is why it must be removed here.

Continuing the derivation, we take the standard Keplerian orbital equation for df_p/dt (Murray & Correia 2010a, their equation 32) evaluated at $f_p = \pi/2 - \omega_p$:

$$\frac{df_p}{dt} = \frac{2\pi [1 + e_p \sin(\omega_p)]^2}{P_p (1 - e_p^2)^{\frac{3}{2}}}, \quad (10)$$

where we have approximated $P_p \simeq P_p(1 + 1/P_\omega)$. Combining equations (8) and (9) gives us the oscillation term

$$T_{\text{PTV}} = \int_{t_0}^t dP_p = \int_{t_0}^t \left(\frac{dt}{df_p} - \frac{P_p}{P_\omega} \right) d\omega_p, \quad (11)$$

which, after inserting equation (10), becomes

$$T_{\text{PTV}} = -\frac{P_b}{P_\omega} \int_{t_0}^t \left(\frac{(1 - e_p^2)^{\frac{3}{2}}}{(1 + e_p \sin[\omega_p(t)])^2} - 1 \right) dt, \quad (12)$$

where the negative sign accounts that this is time gained or equivalently an apparent shortening of the planetary period, and applies for prograde precession. The quantity T_{PTV} represents an oscillation

of the location of possible transits with time. We give an example of its effect through application to a demonstration simulated system in Section 2.2.

2.1.3 Combined TTV limits – practical use

Equations (7) and (12) can be combined to provide limits on the TTVs of transiting coplanar circumbinary planets. At a given epoch, T_{PTV} represents the offset around some zero-point that the range of possible transit times would be centred around, whereas T_{GTV} represents the extent of the range around this offset. We present constraints here for practical use, in the situation where one or more transits have been detected, and limits need placing on the times of as yet undetected transits. A period must be estimated, either from the separation of two transits (or fractions of this) or by using a succession of trial periods. In the case where only one or two transits are known, as we do not know where in the possible transit range the transit falls we must use double the range to cover all possible times, giving the following limits:

$$t_{\min}(i) = t_0 + iP_p + T_{\text{PTV}}(t_0 + iP_p) - T_{\text{GTV}}(t_0 + iP_p) \quad (13)$$

and

$$t_{\max}(i) = t_0 + iP_p + T_{\text{PTV}}(t_0 + iP_p) + T_{\text{GTV}}(t_0 + iP_p), \quad (14)$$

where t_0 represents the time of first transit, and i an index for the orbit under consideration (each orbit may contain more than one transit, though in practice this is unusual). The quantities t_{\min} and t_{\max} represent the minimum and maximum times between which possible undetected transits must fall within on each orbit, for the case of one or two known transits.

Over short ($\ll P_\omega$) time-scales T_{GTV} is the dominant contribution (in some systems, such as those with low-eccentricity planets, it is always so), and T_{PTV} may be neglected. Using the maximum possible value of T_{GTV} (by setting $\omega_p = 3\pi/2$ in equation 7) provides a ‘safe’ (in that the result will always be an overestimate) way of neglecting the time and ω_p dependence of T_{GTV} . Similarly, if little is known about a proposed circumbinary system, parameters in the above equations can be easily approximated with only small and quantifiable errors introduced.

The effects of T_{GTV} and T_{PTV} are shown for a demonstration circumbinary planet in Section 2.2.2.

2.2 Numerical model

2.2.1 Approach

We use a numerical model to test the above analytical framework. The N -body equations of motion were integrated using a fourth-order Runge–Kutta algorithm. Since this integrator does not inherently conserve energy, the total system energy was calculated over time to ensure that it was conserved such that the energy loss fraction remained below approximately 10^{-7} .

To calculate the azimuthal period numerically we averaged the time intervals between the planet passing each of the two boundaries of the projected star orbit. The azimuthal period is the mean of these two averages. An alternative method is to average the interval between system centre of mass crossing times, which will converge to the same value but more slowly because it is only based on one crossing point, not two. Over time, the average interval between consecutive transits will converge to the azimuthal period.

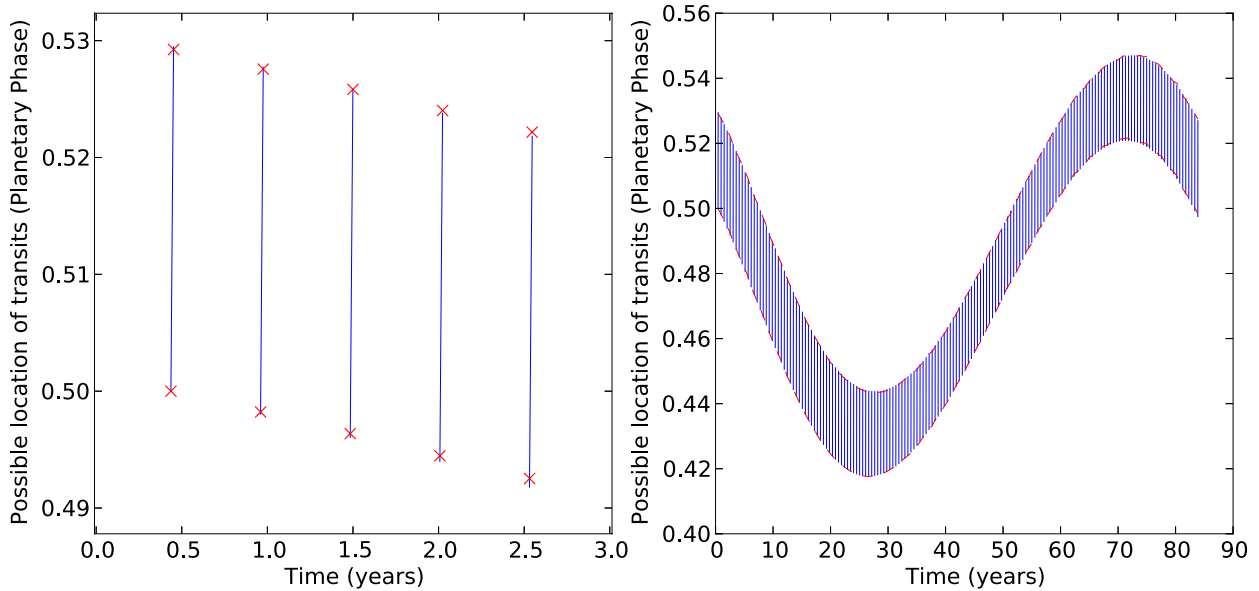


Figure 1. Left: 3 yr and five crossings of a simulated planet. Transits must occur on the lines. The crosses represent the predicted maximum and minimum time for each crossing region derived from our analytical equations. The length in phase of each line represents T_{GTV} , while the shifting of the lines in phase represents T_{PTV} . The phase is calculated through phase folding over the planetary azimuthal period (191.5 d). The starting epoch $t = 0$ is arbitrary, as are absolute values of the phase. Right: as left for a full planetary precessional period. The dashed line shows the analytical equation prediction, realigned with the numerical model every 3 yr (chosen as a representative length for an observing campaign.) Realignment is justified as this is how the equations would be used in practice, with a single detected event representing a zero-point to which the equations would be aligned.

2.2.2 Demonstration

We here apply the numerical and analytical models to a simulated system (chosen from the simulations of Section 3 as a system with a typical error) to demonstrate the effects of the derived timing variations. This system has a binary star with period 14.1 d, eccentricity 0.13, stellar masses of 1.22 and 1.07 M_{\odot} and argument of periape 282.3. The planet has azimuthal period 191.5 d and eccentricity 0.16, leading to a precessional period for the planet of 84.2 yr from the numerical model. Fig. 1 shows the potential locations of planetary transits derived from the numerical model, using times of potential transit phase-folded at the above azimuthal period. Potential transits must occur on each solid line. The variations seen are discussed in Sections 2.2.3 and 2.2.4.

2.2.3 Geometrical timing variations – Effect I

The Effect I geometrical timing variations introduced in Section 1 and derived in Section 2.1.1 arise from the significant motion of the host binary stars. The planet can take several days to traverse the full extent of the binary orbit, and it is during this time that transits will occur. The TTVs, given by equation (7), can therefore be very large. By considering circular orbits and solar-mass stars, equation (7) can be approximated by $T_{\text{GTV}} \approx (P_p P_b^2)^{1/3} / (2\pi)$, with periods in days, which demonstrates the size of the TTVs and their period dependence.

This geometrical contribution to the TTVs corresponds to the length of the lines in Fig. 1. The magnitude of the Effect I term itself oscillates with the precession period of the planet, due to the changing speed of the planet at crossing, as different regions of its eccentric orbit line up with the observer.

2.2.4 Precessional timing variations – Effect II

The other variation, an oscillation in phase or equivalently oscillation in apparent period, is due to the precession of the planet causing transits to correspond to different phases, as seen in Fig. 1 (right). The oscillation is in particular caused by the changing instantaneous effect of the precession on a planet in an eccentric orbit. This is different to the contribution of precession in the Effect I geometrical case, which varies T_{GTV} due to the changing planetary velocity. The Effect II precessional variation becomes significant over time-scales approaching the planetary precessional period, typically decades. The amplitude of this variation is strongly dependent upon the planetary precessional period and eccentricity.

3 RESULTS

3.1 Set-up

The accuracy of the model of Section 2.1 was tested using the numerical model (Section 2.2) applied to a simulated distribution of 1000 single-planet circumbinary systems, 799 of which were stable over 1200 yr (longer than the maximum planetary precession period found, and significantly longer than the majority). A more thorough stability analysis was not deemed necessary for the purposes of testing the equations in this paper. The binary star periods and eccentricities were taken from Halbwachs et al. (2003), which presented an unbiased distribution taken from radial velocity surveys, expanding upon the work of Duquennoy & Mayor (1991). The primary star masses were taken from the Kepler catalogue of all stars monitored, using an empirical calibration from Torres (Torres, Andersen & Giménez 2010) to calculate the mass based on the metallicity, effective temperature and $\log g$. The secondary star mass was determined using the mass ratio distributions found

in Halbwachs et al. (2003), for binaries with periods less than and greater than 50 d. The radii of the stars were unimportant for this test.

For the planets, since no circumbinary planet distribution is known as yet, the period and eccentricity distributions were taken from data for planets orbiting single stars. Only radial velocity data were used to avoid the bias towards small periods seen in transit surveys. The planet was taken as a massless test particle, as its mass has a minimal effect on the dynamics. The planet radius was also unimportant for this simulation, as it has no effect on the dynamics. For each circumbinary system the minimum planet period was four times that of the binary, as a rough stability constraint (Holman & Wiegert 1999), although some systems still proved to be unstable (particularly those with high eccentricities). The maximum planet period was set at 500 d, long enough that TTVs in such systems are unlikely to be of interest in the near future. All systems were exactly coplanar. Each of these systems was integrated numerically over its expected precession period (calculated from the equation of DB) with a time-step of 30 min. The system's azimuthal period was then calculated from the time it took the planet to orbit the system centre of mass on average.

To test the analytical model we used equations (7) and (12) to predict the limits on possible transit time of the simulated planets. The precession period was split into 3-yr baselines (chosen as the length of a representative observing campaign). At each of the 3-yr baseline for each system, the predicted and numerical limits were initially aligned (as would be the case when detecting the first transit of a candidate planet) and then the system and predicted limits were allowed to evolve. At each crossing, the deviations between the upper analytical and numerical limits and lower analytical and numerical limits were averaged, and the same averaged for all crossings within each of the 3-yr baselines.

3.2 Test results

Results are represented as a percentage of the numerically integrated crossing time found at each planetary crossing. As such, an error of 100 per cent represents analytically predicted transit limits which are misaligned by one crossing time on average. Fig. 2 shows the histogram of percentage errors found for the 799 stable systems. The peak shows an error of 0.4 per cent. The median error is 0.84 per cent. For clarity, 43 systems are not shown in Fig. 2. These represent badly predicted single systems, with percentage errors higher than 20 per cent (four of them have errors over 100 per cent). These larger error systems are discussed in Section 4.

3.3 Application to Kepler-16b, -34b and -35b

The numerical model was applied to the known systems Kepler-16b, -34b and -35b, and times of possible transit were extracted. We find azimuthal periods of 227.06, 283.13 and 127.30 d for Kepler-16b, -34b and -35b, respectively. These are slightly offset from those found by LL. These are compared to Keplerian periods from the respective discovery papers of 228.78, 288.82 and 131.46 d (Doyle et al. 2011; Welsh et al. 2012). We note that care must be taken regarding the different reference frames parameters for these planets can be published under, and also regarding the instantaneous and highly variable nature of many of the usual planetary parameters. Fig. 3 shows the potential locations of planetary transits derived from the numerical model, using times of potential transit phase-folded at the above azimuthal periods. Potential transits must occur within the thick band for each planet. The thickness of each band

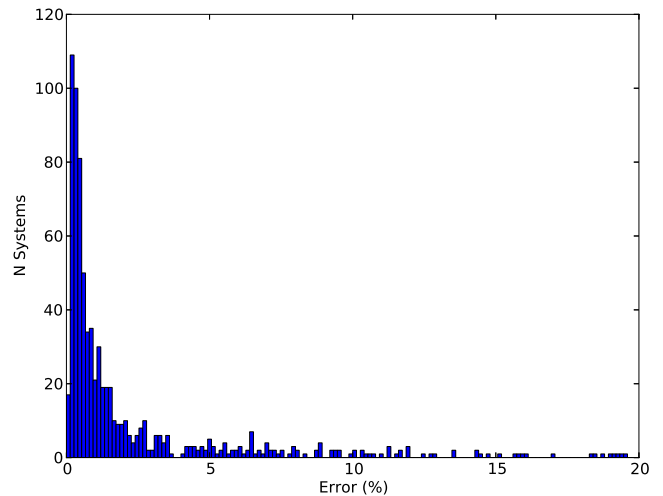


Figure 2. The error in comparing simulated numerical limits on the possible transit locations of 756 systems to the predictions of combining equations (7) and (12). The difference between the analytical and numerical models is expressed as a percentage of the numerical planet crossing duration at each crossing. For clarity, 43 additional systems with errors greater than 20 per cent are not shown. Four of these systems have errors over 100 per cent.

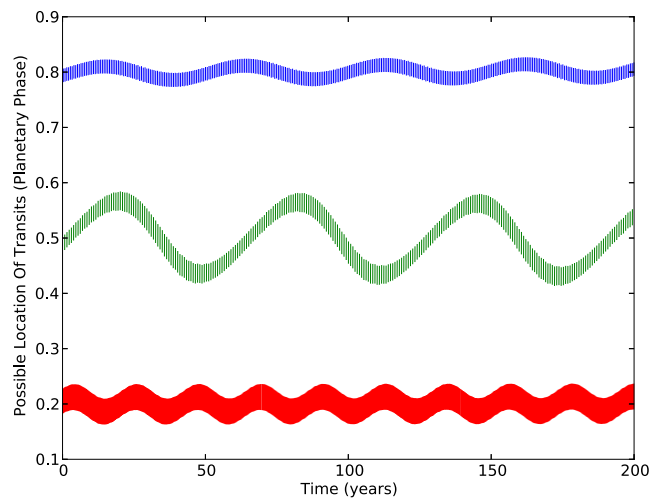


Figure 3. The variation in planetary phase of potential transit times, derived from the numerical model. Transits must occur within the thick bands. From top to bottom, the lines show Kepler-16b, -34b and -35b. The phase is calculated using the planetary azimuthal period in each case. Absolute values of the phase are arbitrary. The starting epoch $t = 0$ is also arbitrary.

represents the Effect I, geometrical timing variation, and the oscillation in phase of the band represents the Effect II, precessional variation. The amplitude of this Effect II variation is strongly dependent upon the planetary precessional period and eccentricity. The period of the Effect II oscillations is equivalent to the planet's precessional period, ~ 48 , ~ 63 and ~ 21 yr for Kepler-16b, -34b and -35b, respectively.

Whilst the previous large-scale test used massless test particles, in this application the planet masses were included in the N -body code. To demonstrate that the planet mass has only a small effect on the transit times, we also simulated the Kepler planets with zero mass. The transit times of the mass and massless simulations were compared over a 200 yr period in blocks of 3 yr. On average

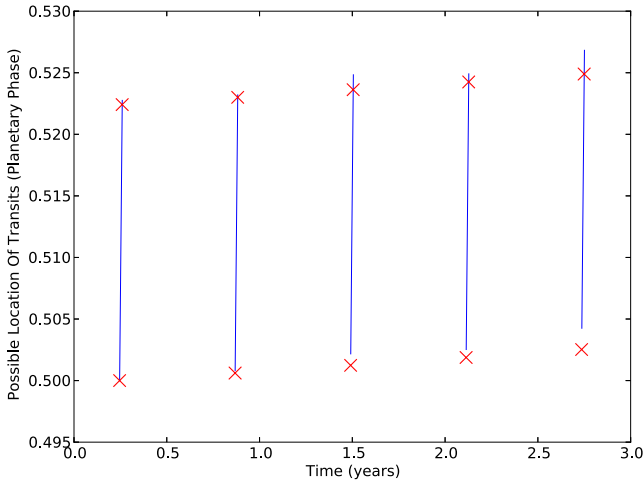


Figure 4. A typical 3-yr region of the Kepler-16b curve of Fig. 3. Transits must occur on the lines. The crosses represent the predicted maximum and minimum time for each crossing region derived from our analytical equations. The length in phase of each line represents T_{GTV} , while the shifting of the lines in phase represents T_{GTV} . Absolute values of the phase are arbitrary. The starting epoch $t = 0$ is also arbitrary.

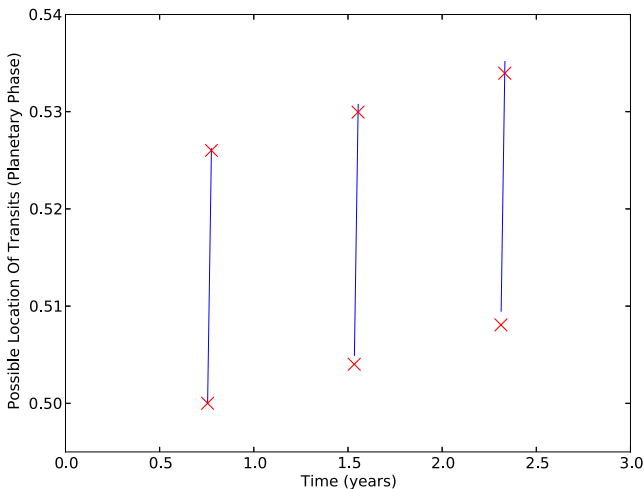


Figure 5. As Fig. 4 for Kepler-34b.

the difference, as a percentage of the TTV range, was only 3.6, 0.8 and 0.7 per cent for Kepler-16b, -34b and -35b, respectively. Future work may include updated equations that incorporate the planet mass, but this will likely only be beneficial for very massive circumbinary planets.

A typical 3-yr region is shown for each planet in Figs 4–6, with the analytical model prediction for each crossing. We note the slight secondary oscillation in Fig. 4. This is an additional dynamical effect likely due to a non-Keplerian effect of the host binary, and is stronger for Kepler-16b than for -34b or -35b. We do not attempt to predict this effect in this work.

4 DISCUSSION

4.1 Overview

We have derived and validated a fast and simple to implement framework for placing limits on the possible locations of transits for a transiting coplanar circumbinary exoplanet. These variations can

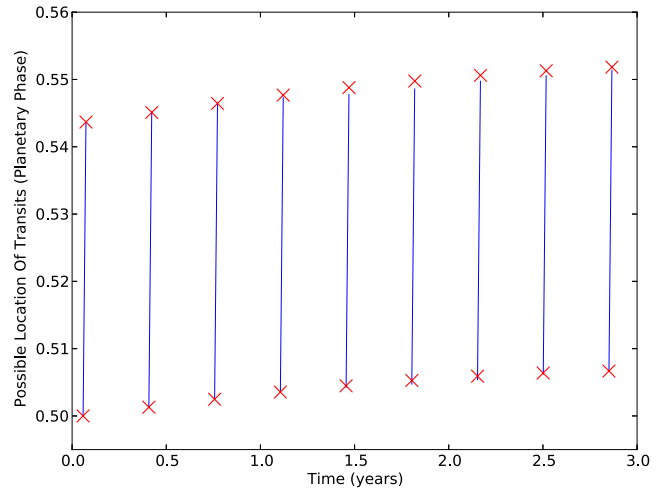


Figure 6. As Fig. 4 for Kepler-35b.

be split into two parts – Effect I, geometrical, caused by the changing positions of the binary stars as they orbit, and Effect II, precessional, caused by the long-term precession of the planet’s orbit. With the likelihood of future searches for circumbinary exoplanets high, and the possibility of discovering such planets in the extant data from previous surveys, being able to place limits on the location in time of potential signals is particularly useful.

4.2 Accuracy

Fig. 2 shows the accuracy of equations (7) and (12) in predicting the possible times of transit of coplanar circumbinary planets – a median percentage error of 0.84 per cent of the planet crossing time across the test set of 799 stable systems, over 3 yr of observations. This can be used as an error when using equations (13) and (14) to predict possible times of transit, where the percentage error should be applied to both t_{max} and t_{min} . We note that our stated errors depend on the time baseline covered – they will be reduced for baselines lower than 3 yr, and increased for those higher. The stated errors should, however, be indicative for a general observing campaign. Limitations on the accuracy arise primarily from non-Keplerian effects (beyond simple constant precession of the planet’s orbit, which we account for). This is demonstrated by the 43 systems with errors greater than 20 per cent, including four with errors greater than 100 per cent. These, and the scattered systems found at over 5 per cent in Fig. 2, are systems which appear to be stable but which show strong dynamical effects we have not accounted for, such as shorter period additional oscillations of ω_p or other effects we do not investigate here. The underlying dynamics behind these are beyond the scope of this paper. Encouragingly, it seems that such effects are strong only in a small minority of cases – the analytical model missed the possible transit range entirely in only 0.5 per cent of the tested stable systems.

4.3 Applications

We anticipate that equations (7) and (12) (and in practice equations 13 and 14) will prove useful particularly for current and future searches for circumbinary planets. They provide a link between our theoretical knowledge of a circumbinary planetary system and the observational transit signatures which may arise from it, without requiring complex modelling or N -body integrations. This can be

used to place limits on the potential transit times of candidate planets around a binary star, for the purpose of constraining searches for the transits of unknown planets. As a specific example, equations (13) and (14) can be used to set the parameters Δ_{\min} and Δ_{\max} in the QATS search algorithm (Carter & Agol 2013). Importantly, this analytic framework can be used on systems where detailed knowledge of the component stars and orbital parameters is lacking, something impossible for N -body models. Full use of equations (13) and (14) requires knowledge of the binary system, specifically the individual stellar masses, binary orbital eccentricity, argument of periaapse and binary period, as well as the argument of periaapse and eccentricity of the planet (while the planetary period is involved, we envisage that for general searches for unknown planets a series of trial periods would be used). Lacking some or all of these details, it is possible to make useful conclusions through using simplifying assumptions – taking $M_2 \ll M_1$ for example removes the need for knowledge of the stellar masses while only overestimating the Effect I timing variation limit by at most a factor of 2 (i.e. placing loose but still useful limits on transit timing).

We repeat that it is possible in general to neglect the time and ω_p dependent part of T_{GTV} (by setting $\omega_p = 3\pi/2$, as the value which gives the maximum value of T_{GTV}). It is also possible for low-eccentricity planets to neglect T_{PTV} . This makes equations (13) and (14) simply a constant limit on the TTV of a planet. These additional terms are however included in this work so that they can be utilized if necessary, particularly for highly eccentric planets or those whose precessional periods approach the baseline of observations used. Note that equations (13) and (14) represent double the range of transit times predicted by equations (7) and (12), as it would not be known where in this range a first detected transit fell.

These equations are also useful in reverse for making first estimates of planet parameters using the observed transit variations of a newly discovered planet candidate. In this situation, the planet azimuthal period must be estimated using the mean transit interval. With this, the maximum observed transit timing variation around this period can be obtained. Neglecting T_{PTV} , this represents a lower limit on equation (7). In the situation where the binary period, eccentricity and argument of periaapse are known through the binary light curve, this gives a constraint on a combination of the planet eccentricity, argument of periaapse and the binary mass ratio. The geometrical contribution T_{GTV} is only weakly dependent on the planet eccentricity for moderate eccentricities, so by setting $e_p = 0$ an approximate lower limit can be found on the binary mass ratio (for $e_p = 0.2$ this approximation has an error of at most ~ 20 per cent, depending on the precise value of ω_p). Conversely, if the lower limit on T_{GTV} found from the observed transits is especially high for the known binary parameters, this is an indication of high planetary eccentricity. Such constraints can be of use when attempting to find best-fitting orbital solutions for these systems.

In the situation where for example only a few transits are detected, and the orbital solution is degenerate or poorly constrained (such that N -body integration is unfeasible), these expressions can be used for placing limits on the time period for which an object should be surveyed from the ground to detect future transits. This makes such follow-up work much more efficient, and becomes relevant when continuous space-based observations are not available.

4.4 Observational considerations

We summarize here some issues which have become apparent affecting observational searches for circumbinary exoplanets. While this paper aims to reduce the difficulty caused by TTVs, these other

limitations to detection of circumbinary planets remain and should be noted.

Azimuthal period. This is the time which on average the planet takes to traverse 2π rad in a fixed reference frame – i.e. the time interval between successive conjunctions. It is offset from, for example, the Keplerian period which can be derived from the planet's semimajor axis and the binary mass. In LL it is shown that the azimuthal period is shorter than the Keplerian orbital period for circumbinary planets. The effect of this can be seen in many of the published transiting circumbinary planets so far. If we take the observed times of transit of these planets and estimate a period from the mean transit interval (which is equivalent to the azimuthal period), the estimated period is generally found to be a few days under the published Keplerian period. This is not an error, but a mark of the difference between the azimuthal period and Keplerian period that LL mention. The effect is clear for Kepler-16b: the maximum TTV at the published Keplerian period (228.78 d) is ~ 13 d, but at the azimuthal period we find (225.72 d), it is ~ 4.5 d, significantly lower. This azimuthal period is the important quantity when considering circumbinary planets from an observational perspective.

Non-coplanarity. If a circumbinary planet is not close to coplanarity with its host binary (such that it is within a few degrees of the binary orbital plane), then due to the motion of the binary stars it will often ‘miss’ them while crossing, exhibiting transits only on some orbits and again making detection much less likely. This constraint is relaxed for binary stars where the mass of one star is much greater than that of its companion (such that the more massive star's orbit is smaller than its radius) or for contact binaries. Furthermore, for systems that are not exactly coplanar, the precession of the planetary orbit will take it in and out of a transiting configuration. This is the case for Kepler-16, where the transits across the larger star A are predicted to cease in early 2018 and return in approximately 2042.

Eccentricity. As part of the source of TTVs of circumbinary exoplanets is due to precession of the planet's orbit, highly eccentric planets will show more variations. While this does not reduce their detection chances as much as the above points, it increases the difficulty caused by these variations, further ‘blurring’ the planet's transit signal. The ‘blurring’ effect of eccentricity is then scaled by the period of the precession of the planet's orbit. Planets that precess faster will experience more transit timing variations over a given time-scale.

5 CONCLUSION

(i) There are two key contributions to the timing variations affecting transits of circumbinary planets. These are geometrical, Effect I, from the motion of the binary stars, and precessional, Effect II, from the precession of the planet's orbit. Other contributions, from for example other planets in the system, are generally on the order of minutes or less in amplitude and negligible compared to these.

(ii) We have derived and validated an analytic framework to quickly estimate each of these terms, for a planet coplanar with its host binary.

(iii) This can be used to place limits on the location of possible transits. In particular, the equations can be approximated using minimal knowledge of the system (in contrast to a more detailed numerical integrator), making them useful for searching data sets for transits of such planets or in reverse making first estimates of parameters using the observed transit variations. Specifically, full use of the equations requires the individual stellar masses, binary

eccentricity, argument of periapse and binary period, as well as the period, argument of periapse and eccentricity of the planet. It is simple to approximate the parameters or use trial values where necessary, as described at various points above.

(iv) We have also summarized some observational issues which have become clear affecting the prospects of detection of circumbinary planets.

ACKNOWLEDGEMENTS

The authors are grateful for the useful comments of an anonymous referee, which helped improve the paper. DVM is funded by the Swiss National Science Foundation. AHMJT is a Swiss National Science Foundation fellow under grant number PBGEP2-145594.

REFERENCES

- Armstrong D. et al., 2012, *A&A*, 545, L4
 Carter J. A., Agol E., 2013, *ApJ*, 765, 132
 Doolin S., Blundell K. M., 2011, *MNRAS*, 418, 2656 (DB)
 Doyle L. R. et al., 2011, *Sci*, 333, 1602
 Duquennoy A., Mayor M., 1991, *A&A*, 248, 485
 Farago F., Laskar J., 2010, *MNRAS*, 401, 1189
 Gong Y.-X., Zhou J.-L., Xie J.-W., 2012, *ApJ*, 763, L8
 Halbwachs J. L., Mayor M., Udry S., Arenou F., 2003, *A&A*, 397, 159
 Holman M., Wiegert P., 1999, *AJ*, 117, 621
 Jaime L. G., Pichardo B., Aguilar L., 2012, *MNRAS*, 427, 2723
 Kane S. R., Hinkel N. R., 2012, *ApJ*, 762, 7
 Lee J. W., Kim S.-L., Lee C.-U., Lee B.-C., Park B.-G., Hinse T. C., 2013, *ApJ*, 763, 74
 Leung G. C. K., Lee M. H., 2013, *ApJ*, 763, 107 (LL)
 Meschiari S., 2012a, *ApJ*, 752, 71
 Meschiari S., 2012b, *ApJ*, 761, L7
 Murray C., Correia A., 2010a, in Seager S., ed., *Exoplanets*. The University of Arizona Press, Tucson, p. 17
 Murray C., Correia A., 2010b, in Seager S., ed., *Exoplanets*. The University of Arizona Press, Tucson, p. 19
 O'Malley-James J. T., Raven J. A., Cockell C. S., Greaves J. S., 2012, *Astrobiology*, 12, 115
 Orosz J. A. et al., 2012a, *ApJ*, 758, 87
 Orosz J. A. et al., 2012b, *Sci*, 337, 1511
 Pelupessy F. I., Zwart S. P., 2012, *MNRAS*, 420, 1503
 Pichardo B., Sparke L. S., Aguilar L. A., 2005, *MNRAS*, 359, 521
 Pichardo B., Sparke L. S., Aguilar L. A., 2008, *MNRAS*, 391, 815
 Pollacco D. L. et al., 2006, *PASP*, 118, 1407
 Prsa A. et al., 2011, *AJ*, 141, 83
 Schwamb M. E. et al., 2012, *ApJ*, 754, 129
 Slawson R. W. et al., 2011, *AJ*, 142, 160
 Torres G., Andersen J., Giménez A., 2010, *A&AR*, 18, 67
 Welsh W. F. et al., 2012, *Nat*, 481, 475
 Wheatley P. J. et al., 2013, in Saglia R., ed., *EPJ Web of Conferences*, Vol. 47, Hot Planets and Cool Stars. EDP Sciences (<http://dx.doi.org/10.1051/epjconf/20134713002>)
 Winn J., 2010, in Seager S., ed., *Exoplanets*. The University of Arizona Press, Tucson, p. 57

This paper has been typeset from a $\text{\TeX}/\text{\LaTeX}$ file prepared by the author.